Arch. Min. Sci. **63** (2018), 2, 321-334

Electronic version (in color) of this paper is available: http://mining.archives.pl

DOI 10.24425/122450

JANUSZ JURASZEK*[#]

STRAIN AND FORCE MEASUREMENT IN WIRE GUIDE

POMIAR ODKSZTAŁCEŃ I OBCIĄŻEŃ W LINIE PROWADNICZEJ

The paper presents a new method for measuring the strain and load of wire ropes guide using fiber optic sensors with Bragg gratings. Its principle consists in simultaneous fiber optic measurement of longitudinal strain of the rope and transverse strain of the bolt fixing the rope. The tensometric force transducers which have been used so far were only able to determine the load in the head securing the rope through an indirect measurement using a special strain insert. They required calibration, compensation of temperature changes, as well as periodic checking and calibration. The head fastening the rope required significant design changes. Measurement based on fiber optic sensors does not have these drawbacks and is characterized by a much higher accuracy and safety of measurements, because the working medium is light. The fastening head does not change. The measurement of the rope load may be based on the change of strain value or indirectly by means of measuring the deflection of the bolt fixing the rope holder. The proposed solution consists in placing the optical fiber with Bragg grating inside the bolt. It enables continuous measurements with a frequency of 2 kHz. A special test bench was built at the Research and Supervisory Centre of Underground Mining. Testing on guide ropes was carried out in a mining hoist in the Piast mine.

Keywords: strain, load,wire, fiber optic sensor

W pracy przedstawiono nową metodę pomiaru odkształceń i obciążeń lin stalowych za pomocą czujników światłowodowych z siatkami Bragga. Istota jej polega na jednoczesnym światłowodowym pomiarze odkształceń wzdłużnych liny i poprzecznych sworznia mocującego linę. Stosowane do tej pory tensometryczne przetworniki siły umożliwiały wyznaczanie jedynie obciążenia w głowicy mocującej linę poprzez pośredni pomiar za pomocą specjalnej wkładki odkształceniowej. Wymagały one kalibracji, kompensacji zmian temperatury, oraz okresowego sprawdzania i wzorcowania. Głowica mocująca linę wymagała znacznych zmian konstrukcyjnych. Pomiar oparty na czujnikach światłowodowych nie posiada tych niedogodności i odznacza się znacznie większą dokładnością i bezpieczeństwem prowadzonych pomiarów, gdyż medium roboczym jest światło. Głowica mocująca nie ulega zmianie. Pomiar obciążenia w linie może być oparty na zmianie wartości odkształcenia bądź pośrednio za pomocą pomiaru ugięcia

---

* UNIVERSITY OF BIELSKO-BIAŁA, WILLOWA 2, 43-309 BIELSKO-BIAŁA
FACULTY OF MATERIALS, CIVIL AND ENVIROMENTAL ENGINEERING

[#] Corresponding author: jjuraszek@ath.bielsko.pl

sworznia mocującego uchwyt liny. Zaproponowane rozwiązanie polega na umieszczaniu światłowodu z siatka Bragga wewnątrz sworznia. Umożliwia ono prowadzenie ciągłych pomiarów z częstotliwością 2 kHz. Zbudowano specjalne stanowisko badawcze w Centrum Badań i Dozoru Górnictwa Podziemnego – CBiDGP. Badania testowe na linach prowadniczych przeprowadzono na wyciągu górniczym w kopali Piast.

Słowa kluczowe: odkształcenia, obciążenia lin, światłowodowe czujniki optyczne

1. Introduction

The design codes and specifications determine the mining infrastructure safety and serviceability requirements which are essential in designing these facilities. Owing to the specific difficult conditions such structures operate in, unexpected overloads or structure degradation may deteriorate them over time, sometimes with disastrous consequences. Therefore, real-time monitoring of structures, using a variety of sensors, is becoming increasingly important. Structural health monitoring has been recently a subject of many studies, attempting to utilize these modern technologies (Ou & Li, 2010; Sumitro et al., 2002; Watkins, 2003; Ye et al., 2014; Chan, 2006).

The use of optical fiber strain sensors, such as distributed optical time domain reflectometry (OTDR) sensors, interferometric in-fiber Fabry-Perot (F-P) sensors, or Brillouin optical time domain analyzer (BOTDA), and fiber Bragg grating (FBG), has become increasingly widespread in structural health monitoring (SHM) (Kim et al., 2011; Li et al., 2004; López-Higuera et al., 2011; Mufti, 2002). Notably, the FBG and F-P sensors use the phenomenon of the sensor refractive index of light changing with the change in length of the sensor. Optical fiber sensors are not susceptible to electromagnetic interference unlike the electrical resistance-based ones. Apart from that, optical fiber sensors also feature other advantages over conventional sensors, including relatively small dimensions, high sensitivity and durability, and the ability to measure at remote locations, even several dozens of kilometers away. The FBG sensor is particularly widely used, as it enables measuring different parameters at many locations using one line of FBG sensors (Rizkalla & Tadros, 1994; Udd, 1996; Werneck et al., 2013; Kim et al., 2015; Moyo et al., 2005). Kim et al. (2016) presented the new technique of sensing by embedding an FBG sensor in a tendon hollow king wire, thus using the king wire as both a sensor and a prestressing wire. As reported by Kim et al. (2012, 2016), the measurement of prestressing force and strain in seven-wire steel strands, frequently employed in PSC members, is also possible.

An FBG sensor, a type of distributed Bragg reflector positioned in a short segment of optical fiber, reflects one wavelength and transmits another one by periodic variation in the fiber core refractive index, upon exposure to ultraviolet laser light. The change in the reflected wavelength is the result of a change in such properties of the FBG sensor as temperature or external load. Thus, the relationship between the FBG sensor reflected wavelength and the physical properties enables the physical quantity measurement.

Light wavelengths corresponding to Bragg gratings are reflected, while other wavelengths are transmitted through the gratings. To calculate the reflected wavelength, Equation (1) can be used.

$$\lambda_B = 2n_{eff}\Lambda, \tag{1}$$

where n_{eff} and Λ are the effective refractive index of the grating of the optical fiber and the grating period, respectively (Zhou et al., 2003; Hill & Meltz, 1997).

As mentioned above, there are many advantages to FBG sensors. However, being made of a glass-based material, they are also brittle and thus susceptible to damage during installation. A protection of some type, then, is necessary, and this is what Iten (Iten, 2012) studied, comparing the performance of several methods for optical fiber-based sensors protection. As evidenced by testing, the improvement in the maximum strain measurement range of optical fiber is obtained by using double protection layers featuring a hard plastic external casing and an infill of soft plastic separating it from the optical fiber itself.

2. The research subject and description of the measurement bench

The purpose of the research was to develop a new method of continuous measurement of longitudinal strain of a steel guide rope installed in the shaft hoist during its operation with simultaneous measurement of the load in the line by measuring the lateral deformation of the bolt fixing the rope in the head. This need stems from the fact that the guide rope in the shaft works in the conditions of high concentration of dust, grease and moisture, and mounting the sensors directly on the rope is difficult due to the passing vessel. This means that continuous monitoring of the operation of such a rope with conventional measurement methods (electric resistance strain gauge) is not very effective, and for the most common method of rope diagnostics – magnetic method, monitoring of continuous operation becomes impossible.

The subject of the research were guide ropes with a diameter of 42 mm used in the mining hoist of the KWK PIAST mine in Bieruń. The use of rope guidance involves many benefits such as:

- good fatigue life (Hankus, 2000),
- small dimensions allow using the shaft better as a ventilation shaft,
- no interference in the shaft wall – guide ropes do not have to be rigidly attached to the housing,
- good access makes it easy to replace and maintain such ropes,
- reduction of material needed for guiding the vessels.

This solution has several negative aspects:

- due to the conditions in the shaft and the method of fixing the rope, it is very difficult to assess the technical condition of such a rope. This problem will be more widely discussed in this paper,
- the backtwist moment of the rope requires the use of even number of ropes, which are coiled in opposite directions in order to reduce each other,
- this solution requires a deeper shaft, due to the moving load,
- the need to use fender ropes to prevent the vessel from tilting or rotating,
- additional load for the hoist tower.

Hence the necessity of continuous measurement of rope tension and the simultaneous measurement of rope strain and elongation proposed in the paper. A new aspect of the issue is the use of fiber-optic FBG sensors for indirect measurement of load in the rope by measuring the deflection of the fastening bolt with simultaneous measurement of rope strain at a given load. A new unique and comprehensive rope research concept is applied.

The diagram of the mining hoist with guide ropes is shown in Fig. 1.

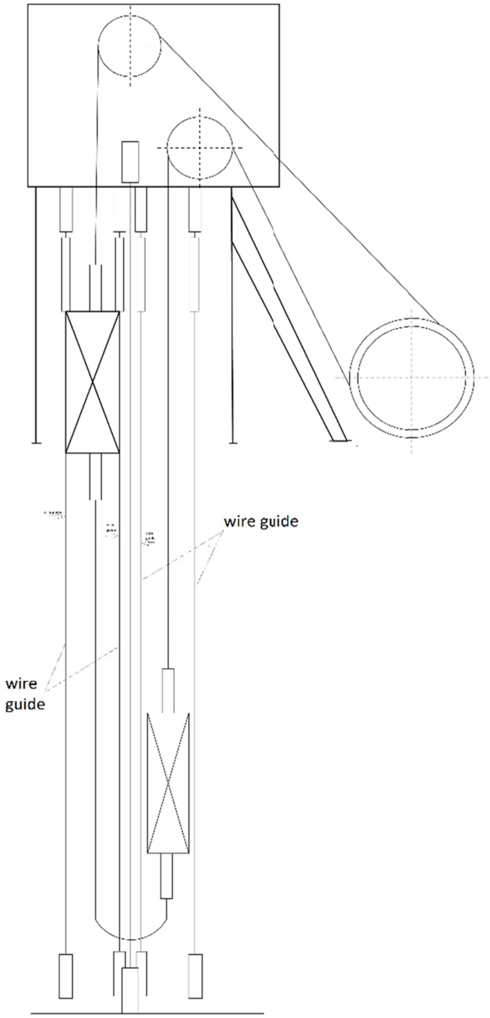

Fig. 1. Cross-section of a mining hoist with the wire guide

The tested rope was therefore exactly the same as the one used in the mining hoist at the Piast mine. It features the following parameters:

- type: full locked,
- diameter: 42 [mm],
- construction: 24Z+10H+12+6+1,
- tensile strength: 1960 MPa,
- wire coating: a grade zinc coated,
- application: guide rope in the mining shaft.

The research was carried out in two stages. In the first laboratory stage, a test bench was constructed, holders fixing optical fiber sensors to the tested rope were designed and a concept for measuring force loads in the rope was developed. It consisted in the fiber optic measurement of deflections of the bolt fixing the rope conical handle in the head so that the design of the head fastening the rope would not change. Numerical simulation of the operation of the bolt in the head securing the rope was carried out using FEM. The bolt was loaded with the maximum force achieved during tests on the testing machine, that is 240 kN. In Fig. 2. the distribution of stresses and strains of the bolt is presented. Based on numerical tests, the position of a fiber optic sensor with a distance of 0.42 R from the axis of the bolt was assumed.

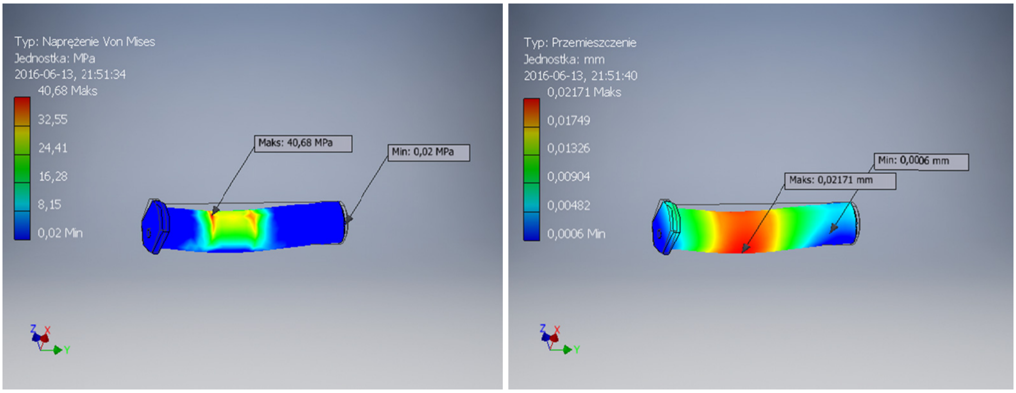

Fig. 2. Stress (left side) and strain distribution in the bolt

A pin prototype was printed using a 3-D printer. Inside the hole of the bolt, a fiber optic sensor with a special pre-tension was sunk in a special material. A laboratory investigation program was then carried out. The layout of the test bench is shown in Fig. 3. The longitudinal section shows the location of the FBG sensor in the bolt and the place of fixing the fiber optic strain sensor with a measuring base of 1000 mm. The second stage of the research included tests on the real object, i.e. guide ropes at the Piast mine.

The load during laboratory tests was applied by means of UPDH 100 s universal testing machine manufactured by MFL SYSTEMS. The research was carried out at the Research and Supervisory Centre of Underground Mining. This machine has a hydraulic drive, a force measurement head type: PA-333X280 bar with an upper measuring range of 1MN and a force measurement accuracy class 0.5. The whole machine is controlled by a computer system. The photo of the measuring station is shown in Fig. 4.

3. Testing methodology

The selection of rope loads was a very important issue. The nominal load resulting from rope guide weights is in the range of 140-150 kN for this type of rope. In the first phase of rope strain testing, a nominal value of 140 kN was adopted and gradually increased to 200 kN and then reduced to the initial value of 140 kN. The essence of the study consists in determining the correlation between changes in strength in the testing machine and the corresponding changes in rope strain (Juraszek, 2013). However, considering the overloads possible in the

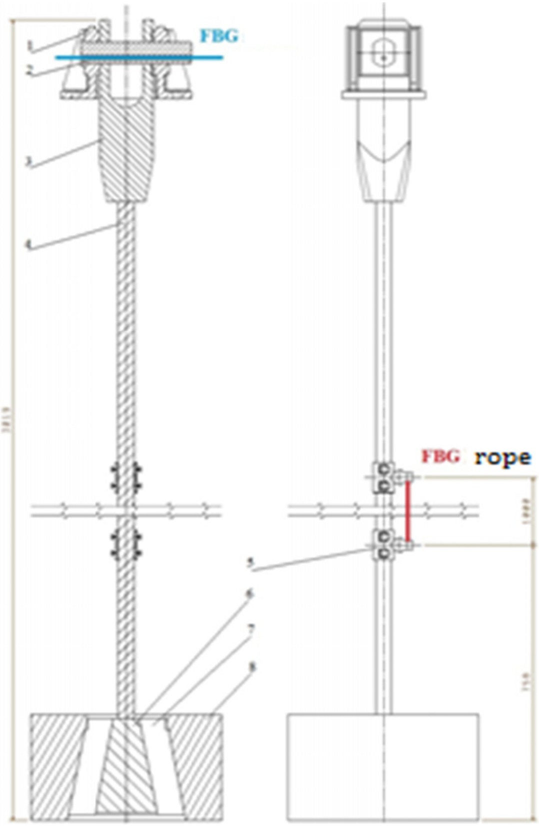

Fig. 3. Layout of the measurement bench: 1 – body, 2 – bolt, 3 – conical handle with eyes, 4 – closed structure rope, 5 – optic fiber holder, 6 – conical rope end, 7 – mount cone, 8 – well

Fig. 4. Laboratory measuring bench

system, the design of the mounting head and bolt is designed for a load of 240 kN. Therefore, in the second phase of research on the experimental bolt, the load was increased to 200 kN and then to 240 kN. It was also important to adopt the lower value of the force to which the system can be relieved so that no looseness occurs. The lowest relief value of the entire system was adopted at 14 kN.

Description of the rope and rope fixing bolt testing

The measurement of bolt deformability was divided into three stages in which the location of the FBG fiber optic sensor relative to the bolt axis changed, while the load for each bolt position was the same. The experimental bolt with the fiber optic sensor was rotated at an angle of 0°, 45° and 90° in relation to the initial position, in which the axis of the fiber optic sensor was placed lowest in relation to the axis of the bolt.

Test I: consisted in loading the rope with 240 kN, then relieving the rope to 20 kN.

Test II: consisted in loading the rope with a force of 200 kN, and relieving it to 140 kN. The entire loading and relieving cycle was repeated 10 times. After the test, the load was released on the testing machine, the obtained results were saved, and the position of the bolt was changed.

Further, the bolt was rotated to a new position, while the entire load and relieve cycle was repeated as for the previous position. The entire testing was recorded using two fiber optic sensors with Bragg grating and a sensor synchronized with the testing machine.

In order to compare the bolt strain and the rope strain, a deformation coefficient was proposed, which determines the relationship between the longitudinal strain of the rope and the lateral strain of the bolt:

$$\varepsilon_l = R_r * \varepsilon_s$$

where:

ε_l — longitudinal strain of the rope,
R_r — correction factor,
ε_s — lateral strain of the bolt.

The setting of the bolt in the 0° position is shown in Fig. 5.

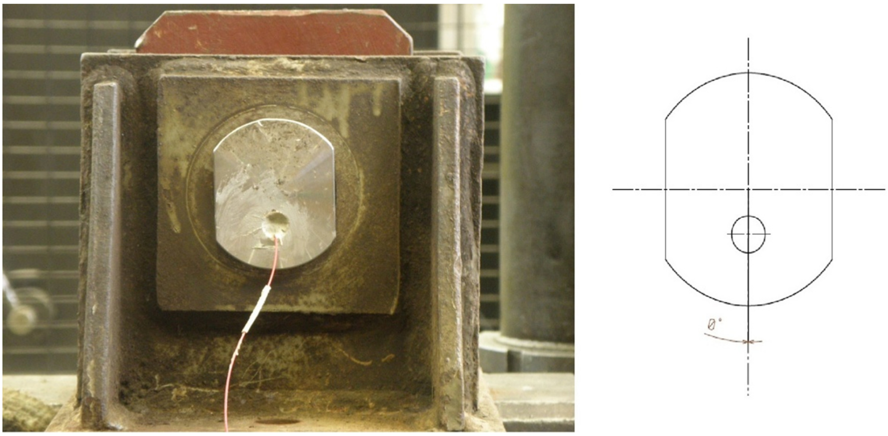

Fig. 5. Test for the bolt position at 0° in the rope mount head

4. Laboratory research results

As a result of the conducted laboratory research, the deformation characteristics of the rope in the load range of 140-200 kN was determined.

The research was conducted using ZD-100 universal testing machine. In Fig. 6 there is a diagram of experimental measurements using FBG optical fiber sensor vertically mounted on the testing machine. SC-01 fiber optic sensor, monitoring the extension of the rope measuring section was connected to FBG Scan 800D optical interrogator, which is also the source of broadband ASE light and measures the Bragg wavelength shift in the transmission spectrum of the FBG sensor. Using the testing machine control panel, you can control the force applied to the rope and simultaneously record it as a function of time. In the tests carried out, the force applied to the rope, from the value of the specified initial tension of 140 kN was increased by 6 kN to a value of 200 kN. At the same time, strain was continuously recorded using a fiber optic system. Each increment of force was translated into the increase of recorded strain of the FBG sensor 300 μstrain. The test results are shown in figures xx. There is a linear relationship between load force and the strain recorded by the FBG sensor. Loading and unloading tests were carried out 40 times and the determined value of the measurement uncertainty did not exceed 2 μstrain. Such a large number of loading and unloading tests also resulted from the need to try a system for sensor mounting to the rope. During the experiments, the temperature was kept as a constant 24C, and thus the strain change can be deemed to result from changing the rope loading force. Fibre optic systems can operate at variable temperature conditions but an adjustment of the measured strain values is necessary in this case. This is possible thanks to fiber optic temperature sensor that sends information about changes in the temperature of the measuring system. The results of stress tests of fiber optic measurement system is shown in Fig. 6. The sensor has a linear characteristics for load range from 0 to 600 kN. Studies were also carried out on a rope attached to the guide rope with an overall length of 750 meters mounted in a coal mine shaft. The rope loading was done using certified cylinders. Loading and unloading characteristics obtained are identical to the characteristics established in the testing laboratory Fig. 7.

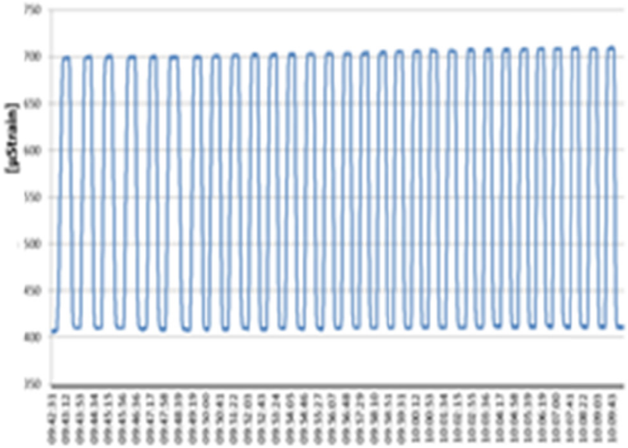

Fig. 6. Rope strain measurement using the sensor

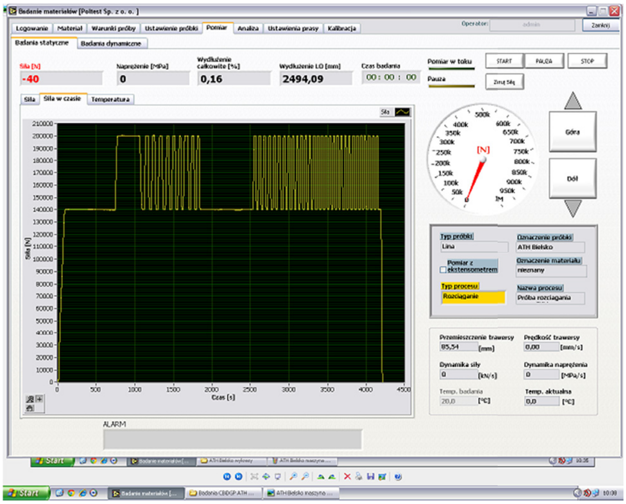

Operator: admin

Siła [N]: -40

Naprężenie [MPa]: 0

Wydłużenie całkowite [%]: 0,16

Wydłużenie LO [mm]: 2494,09

Czas badania: 00 : 00 : 00

Pomiar w toku

Pauza

Typ próbki: Lina

Oznaczenie próbki: ATH Bielsko

☐ Pomiar z ekstensometrem

Oznaczenie materiału: nieznany

Typ procesu: Rozciąganie

Nazwa procesu: Próba rozciągania

Przemieszczenie trawersy: 85,54 [mm]

Prędkość trawersy: 0,00 [mm/s]

Dynamika siły: 0 [kN/s]

Dynamika naprężenia: 0 [MPa/s]

Temp. badania: 20,0 [°C]

Temp. aktualna: 0,0 [°C]

Fig. 7. Stress test – testing machine

The calculation of the level of stress caused by increase in the force by 60 kN – from the level of 140 kN to the level of 200 kN (normal stress related to values obtained on the testing machine during rope testing process: 60,7 MPa). Further research concerned the deformability of the experimental bolt. The strain characteristics of the entire measuring head-bolt system are shown in Fig. 8. It can be seen that after the initial backlash elimination in the system, it works repetitively. The value of the relieved force was 240 kN. This value can occur in the event of an overload or failure. In a real facility, the force occurring in the system should oscillate around 140-150 kN.

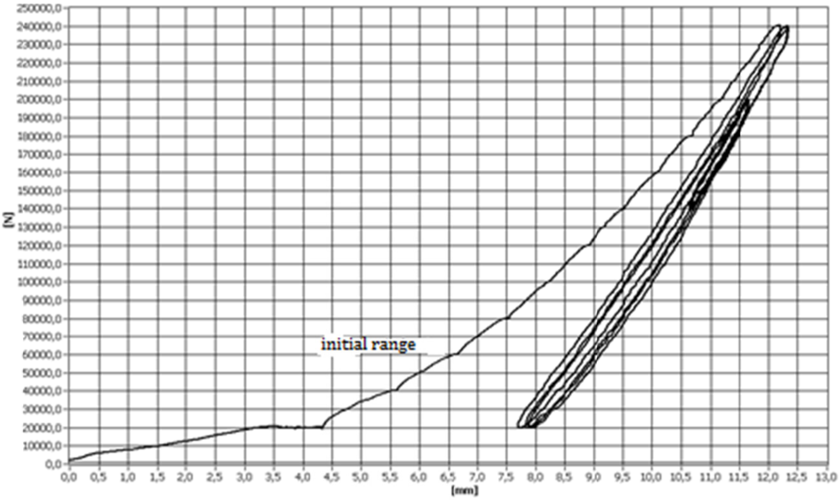

Fig. 8. The curve of rope load coming from the sensor synchronized with the testing machine – 0° pin

It is very interesting from a practical point of view to compare the strain diagrams of the rope and the bolt. They are shown in Fig. 9. The comparison shows that as the strain of the rope increases to 1200 strain, the bolt deformation is similarly increased to 400 strain for the highest value of the loading force. Differences in rope and bolt strain values result from different stiffness and load type. The rope is stretched and the bolt is bent. The relieving process follows in the same way. Next, a cycle of tests was proposed with the average strain value of the rope of 800 strains. A comparative chart for 10 load cycles is given in Fig. 10. For the adopted working point of the guide rope corresponding to the strain of 800, the corresponding bolt strain is 275 strain. The deformation coefficient reaches a value of 2.54. Similar tests were carried out for 45 and 90 degree bolt positions. For 45°, the correction factor is $R_r \approx 5.563$.

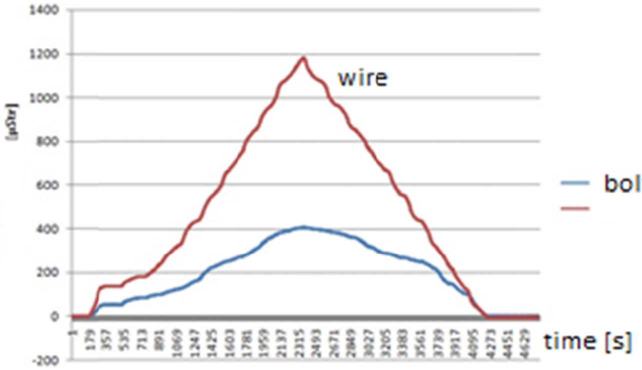

Fig. 9. Load characteristics of the rope and bolt for 1 cycle for test I – 0° bolt position

For 0° and test I the correction factor is $R_r \approx 2.394$. This factor is calculated as the arithmetic average of the ratio of all tests (disregarding the initial and final range, where rope and bolt do not operate in a stable way).

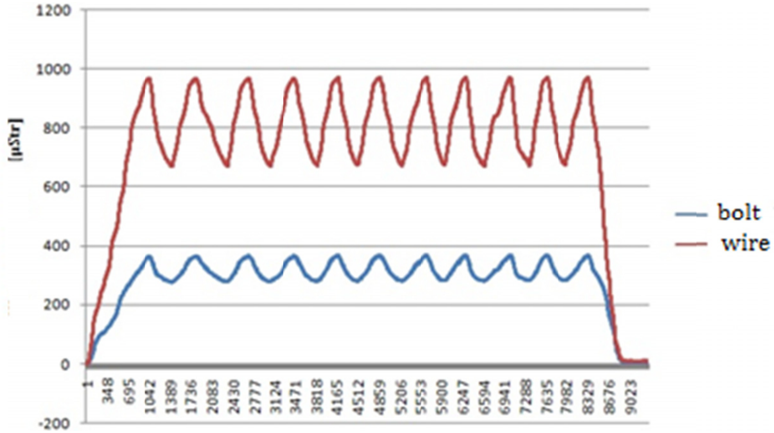

Fig. 10. Load characteristics of the rope and bolt for 10 cycles for test II – 0° bolt

Analysis of the rope-to-bolt deformation ratio, disregarding the initial and final range, indicates that it is constant in a vast range of loads. However, taking into account the rheological properties of the rope, the ratio will change over time as the rope is used. This can be an important information as regards the operation of ropes. The rope-to-bolt deformation ratio is shown in Fig. 11.

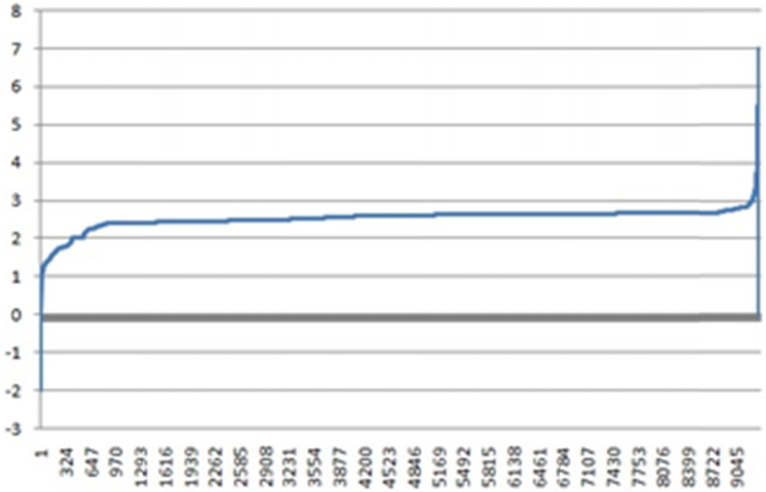

Fig. 11. The ratio of longitudinal strain of the rope to the lateral strain of the bolt for test II – 0° bolt

5. The results of tests carried out on the guide line in the mining shaft hoist

The fiber optic measuring system presented in the paper was installed on the mining hoist at the KWK Piast mine. The system was expanded with a temperature-change correction system and a special low-voltage power system for the optical interrogator and a computer recorder. The FBG 800 optical interrogator enables recording of test results at a frequency of 2 kHz which makes it suitable for dynamic tests. Test guide ropes had installed weights causing their initial tension of 150 kN. Fiber optic sensors were installed on the ropes using specially designed brackets enabling axial adjustment of the sensor. The research involved moving the vessel up and down. At the bottom, there was machine unloading and loading of cargo to be transported up to the surface. Individual trips up and down were recorded. The results of deformation measurements of the rope during loading on the upper level (carcass) and going down are shown in Fig. 12. Loading causes a rope strain of approx. 67.2 strain and moving down causes a lot of vibrations and strain of approx. 46 strain. Similar strain values occur during unloading at the lower level of 67.6 strain. It was presented in Fig. 13.

The most interesting, from a practical point of view, is the change in the values of forces occurring in the guide rope during operation. On the basis of the strain values for the bolt with the fiber optic sensor and the calibration tests, actual values of the forces occurring in the guide rope were determined. They were presented in Fig. 14. The graph shows that the force in the

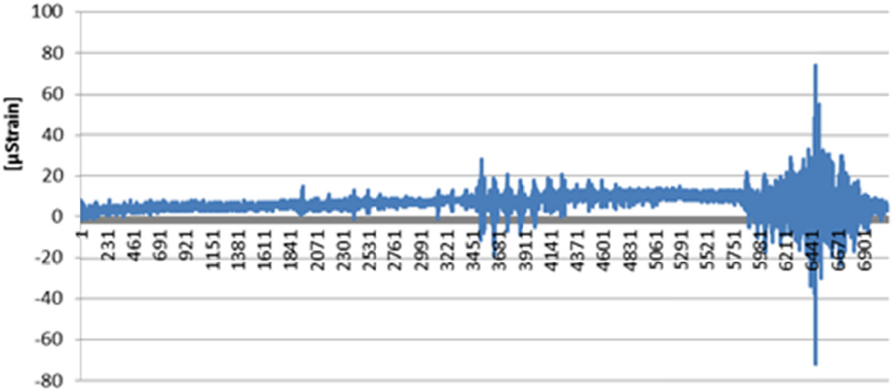

Fig. 12. Strain of the rope during the passage to the lower loading level

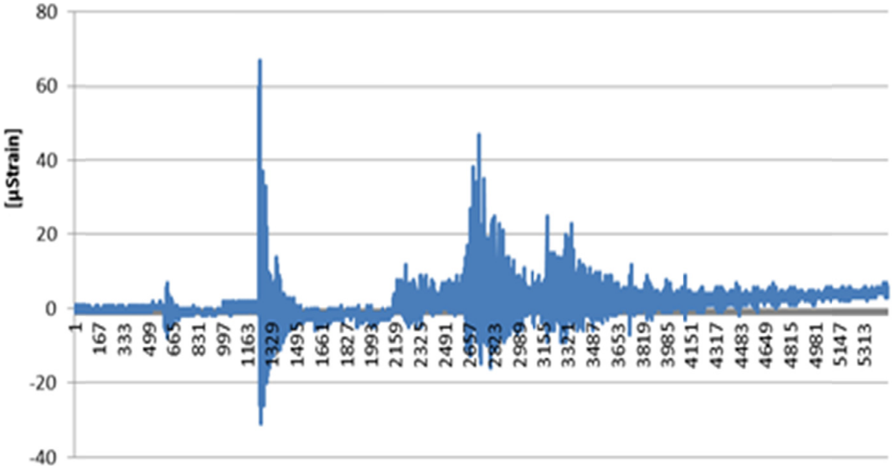

Fig. 13. Unloading of goods at the lower loading level

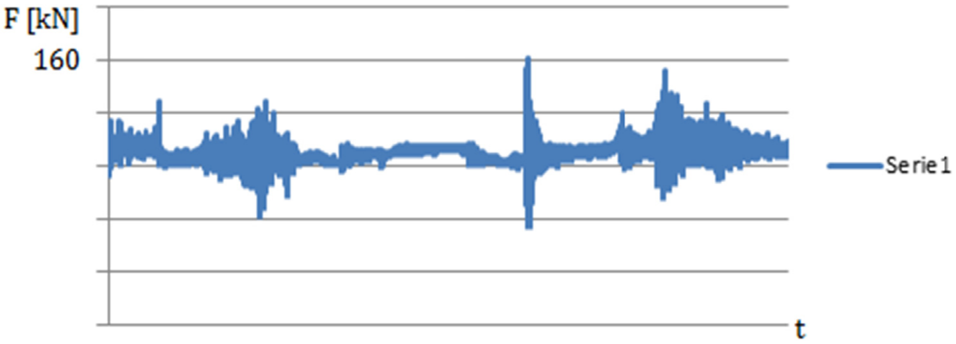

Fig. 14. Actual force values occurring in the guide rope

rope oscillates around the value of 150 kN, with numerous vibrations in the range of 144.3 kN to 160.5 kN. It must be pointed out that while moving the vessel as well as when loading cargo numerous vibrations occurred.

6. Conclusions

The article presents a summary of work on a new fiber optic system which enables monitoring of strain and loads occurring during operation of the ropes in mining shaft hoists. Based on a comprehensive review of theories, methods, technologies and applications based on fiber optic sensors, the following final conclusions can be made:

1. The actual value of force in the guide rope was determined. It ranged from 144.3 kN to 160.5 kN. At the same time, the measurement of rope strain makes it possible to analyze the change in the strain over time during operation with the known rope load. Such comprehensive information has not been available so far. It can be useful when conducting rope fatigue tests based on the actual rope load spectra.

2. The bolt-sensor with accurately installed fiber optic sensor records the force load in the rope. The location of the sensor inside the pin does not necessitate any changes in the design of the head fastening the guide ropes, which makes the proposed solution universal.

3. Due to the unique advantages of fiber optic sensors such as intrinsic safety, significant measurement accuracy, fatigue durability, they should be widely used in monitoring the life cycle of mining infrastructure, including guide ropes.

4. The proposed system of strain and loads monitoring of guide ropes can significantly contribute to increasing the operational safety of transport equipment in mining.

Acknowledgments

We would like to express our thanks to the Research and Supervisory Center of Underground Mining (Centrum Badań i Dozoru Górnictwa Podziemnego – CBiDGP) for the possibility of performing our laboratory tests and to the KWK Piast mine for making it possible to carry out tests on the guide lines of their mining shaft hoist

References

Chan T.H., Yu L., Tam H.-Y., Ni Y.-Q., Liu S., Chung W., Cheng L., 2006. *Fiber Bragg grating sensors for structural health monitoring of Tsing Ma bridge: Background and experimental observation*. Eng. Struct. **28**, 648-659.

Hankus J., 2000. *Budowa i własności mechaniczne lin stalowych*. GIG, Katowice.

Hill K.O., Meltz G., 1997. *Fiber Bragg grating technology fundamentals and overview*. J. Lightwave Technol. **15**, 1263-1276.

Iten M., 2012. *Novel Applications of Distributed Fiber-Optic Sensing in Geotechnical Engineering*. Volume 19-632 VDF Hochschulverlag AG; Zürich, Switzerland.

Juraszek J., 2013. *Innowacyjne, nieniszczące metody badań diagnostycznych*. ATH, Bielsko-Biała.

Kim J.-M., Kim H.-W., Choi S.-Y., Park S.-Y., 2016. *Measurement of prestressing force in pretensioned UHPC deck using a fiber optic FBG sensor embedded in a 7-wire strand*. J. Sens.

Kim J.-M., Kim H.-W., Park Y.-H., Yang I.-H., Kim Y.-S., 2012. *FBG sensors encapsulated into 7-wire steel strand for tension monitoring of a prestressing tendon*. Adv. Struct. Eng. **15**, 907-917.

Kim S.T., Park Y., Park S.Y., Cho K., Cho J.-R., 2015. *A sensor-type PC strand with an embedded FBG sensor for monitoring prestress forces*. Sensors. **15**, 1060-1070.

Kim Y.-S., Sung H.-J., Kim H.-W., Kim J.-M., 2011. *Monitoring of tension force and load transfer of ground anchor by using optical FBG sensors embedded tendon*. Smart Struct. Syst. **7**, 303-317.

Li H.-N., Li D.-S., Song G.-B., 2004. *Recent applications of fiber optic sensors to health monitoring in civil engineering*. Eng. Struct. **26**, 1647-1657.

López-Higuera J.M., Cobo L.R., Incera A.Q., Cobo A., 2011. *Fiber optic sensors in structural health monitoring*. J. Lightwave Technol. **29**, 587-608

Moyo P., Brownjohn J., Suresh R., Tjin S., 2005. *Development of fiber Bragg grating sensors for monitoring civil infrastructure*. Eng. Struct. **27**, 1828-1834.

Mufti A.A., 2002. *Structural health monitoring of innovative Canadian civil engineering structures*. Struct. Health Monit. **1**, 89-103.

Ou J., Li H., 2010. *Structural health monitoring in mainland China*. Review and future trends. Struct. Health Monit. **9**, 219-231.

Rizkalla S., Tadros G., 1994. *First smart highway bridge in Canada*. Concr. Int. **16**, 42-44.

Sumitro S., Jarosevic A., Wang M.L., 2002. *Elasto-Magnetic Sensor Utilization on Steel Cable Stress Measurement*. Proceedings of the First FIB Congress; Osaka, Japan. 13-19 October 2002, p. 13-19.

Udd E., 1996. *Fiber optic smart structures*. Proc. IEEE. **84**, 884-894.

Watkins S.E., 2003. Smart bridges with fiber-optic sensors. IEEE Instrum. Meas. Mag. **6**, 25-30.

Werneck M.M., Allil R., Ribeiro B., de Nazaré F., 2013. *Current Trends in Short-and Long-Period Fibre Gratings*. InTech; Rijeka, Croatia. A guide to fiber Bragg grating sensors; p. 1-24.

Ye X., Su Y., Han J., 2014. *Structural health monitoring of civil infrastructure using optical fiber sensing technology: A comprehensive review*. Sci. World J.

Zhou Z., Graver T.W., Hsu L., Ou J., 2003. *Techniques of advanced FBG sensors: Fabrication, demodulation, encapsulation and their application in the structural health monitoring of bridges*. Pac. Sci. Rev. **5**, 116-121.